Toxicokinetics of crude oil components in Arctic copepods

Ida Beathe Øverjordet[1*], Raymond Nepstad[1], Bjørn Henrik Hansen[1], Tjalling Jager[2], Julia Farkas[1], Dag Altin[3], Ute Brönner[1], Trond Nordtug[1]

[1] SINTEF Ocean AS, Trondheim, Norway
[2] DEBtox Research, De Bilt, The Netherlands
[3] BioTrix, Trondheim, Norway

*Corresponding author: Ida Beathe Øverjordet, ida.beathe.overjordet@sintef.no

Keywords
Toxicokinetics, Body residues, Bioconcentration factors (BCF), polycyclic aromatic hydrocarbons (PAH), water soluble fraction (WSF)

Abstract

The risk of accidental oil spills in the Arctic is on the rise due to increased shipping and oil exploration activities, making it essential to calibrate parameters for risk assessment of oil spills to Arctic conditions. The toxicokinetics of crude oil components were assessed by exposing one lipid-poor (CIII) and one lipid-rich (CV) stage of the Arctic copepod *Calanus hyperboreus* to crude oil WSF (water-soluble fraction). Water concentrations and total body residues (BR), as well as lipid volume fractions, were measured at regular intervals during exposure and recovery. Bioconcentration factors (BCFs) and elimination rates (k_e) for 26 petrogenic oil components were estimated from one-compartment models fitted to the BR data. Our parameters were compared to estimations made by the OMEGA bioaccumulation model, which uses the octanol-water partitioning coefficient (K_{OW}) in QSAR (quantitative structure-activity relationship) predictions. Our parameters for the lipid-poor CIIIs generally agreed with the OMEGA predictions, while neither the BCFs nor the k_es for the lipid-rich CVs fitted within the realistic range of the OMEGA parameters. Both the uptake and elimination rates for the CVs were in general half an order of magnitude lower than the OMEGA predictions, showing an overestimation of these parameters by the OMEGA model.

41 TOC art

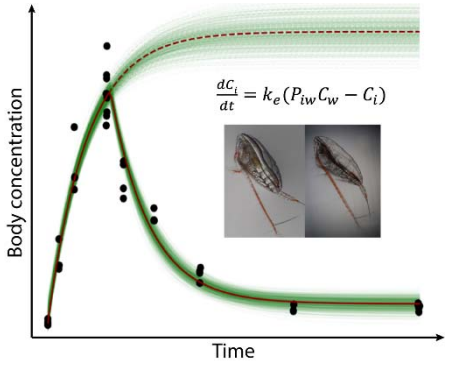

42

1 Introduction

Increased oil and gas exploration and production in Arctic areas, combined with the potential for shipping in previously ice-covered waters, enhance the risk of accidental spills of fuel and crude oils in the Arctic. Both fuel and crude oils consist of a wide range of organic compounds, including polycyclic aromatic hydrocarbons (PAHs), with different physical and chemical properties, like water solubility and lipophilicity. A fraction of these compounds will be present in the aqueous phase of an oil-water dispersion, termed the water-soluble fraction (WSF). The dissolved fraction is believed to be the main driver of oil toxicity due its bioavailability.[1-3] The lipophilicity of organic compounds can be expressed as the octanol-water partitioning coefficient (K_{OW}), with a high K_{OW} indicating a high tendency to partition to the organic phase.

Bioconcentration factors (BCF) are defined as the internal concentration of a compound in an organism in steady state, divided by the concentration in water.[4] Relationships between BCF and K_{OW} are widely used in QSAR (quantitative structure activity relationship) based bioaccumulation modelling to predict environmental fate, bioconcentration potentials and toxicity of organic compounds in risk assessment.[5-8] In QSAR analyses, the BCFs of lipophilic compounds are predicted to equal K_{OW} times the lipid fraction (f_L) of the organism ($BCF=f_L \times K_{OW}$), based on the assumption that lipophilic organic compounds mainly partition to the lipid compartment of the organism.[4, 5, 7] The OMEGA bioaccumulation model by Hendriks *et al.*[6] uses the K_{OW} of organic components, as well as the body mass, lipid fraction and trophic position of the organism to predict uptake and elimination rate constants.

Arctic species differ from temperate species in terms of lipid content, surface-to-volume ratios and basal metabolism,[9] and toxicokinetic parameters obtained from temperate species may not be representative for Arctic conditions.[10, 11] Information on toxicokinetic parameters for oil components in lipid-rich Arctic zooplankton is limited, and the most relevant studies have assessed only a few PAHs.[12, 13] Testing Arctic species is thus vital to calibrate parameters for risk assessment to Arctic conditions. The pelagic copepod *Calanus hyperboreus* is an important source of energy in Arctic marine food webs.[14] They undergo six naupliar stages (NI-NVI) and five copepodite stages (CI-CV) before they moult into adult males or females[15]. From stage CIII they start to build up large discrete lipid reservoirs (lipid sacs), which consist mainly of wax esters used to survive periods of diapause and to fuel gonad maturation and reproduction in early spring.[15-17] The high lipid content of the late stages of *C. hyperboreus* enhances its potential for bioaccumulation of oil components,[12] increasing the risk

of chronic exposure of sensitive tissues during depuration, and of maternal transfer of oil components to developing eggs.[18]

The central position of *C. hyperboreus* in the Arctic food web, as well as its Arctic adaptation, makes it a suitable species for validation of toxicokinetic QSAR models for lipid-rich Arctic zooplankton. We here provide toxicokinetic data and model parameters for 26 crude oil components for two developmental stages of *C. hyperboreus* (CIII and CV). By considering the model parameters of multiple oil components in two stages simultaneously, and comparing these to the predictions from the OMEGA model, we discuss the validity of QSAR predictions for lipid-rich Arctic species in relation to biological and chemical properties.

2 Materials and methods

2.1 Experimental animals

Lipid-rich *C. hyperboreus* CV were collected by net hauls (1000 µm mesh) from r/v Porsild (University of Copenhagen) outside Arctic Station in Qeqertarsuaq (Disko Bay, Greenland) in September 2016. Female *C. hyperboreus* were collected by net hauls from the sea ice at the same location in February 2017. Transport to Trondheim, Norway, was by air freight in thermo-stable containers (55 h and 54 h, 3 – 7 °C and -1 – 3 °C in 2016 and 2017, respectively). Upon arrival, the containers were equilibrated to 2.5 °C before transfer of the *C. hyperboreus* to polystyrene holding tanks (250 L flow-through, 2.5 °C). The CVs were used in the exposure experiment directly after acclimation. The females were transferred to 5 L buckets (20, n=10 in each) for egg collection over 1 week. The eggs were carefully collected from the surface and transferred to polystyrene holding tanks (250 L flow-through, 2.5 °C), where the CIIIs was reared (approx. 15 weeks). The incubation chambers were supplied with microalgae (nominal 55µg C/L; *Rhodomonas baltica* (65% C), *Dunaliella tertiolecta* (10% C) and *Isochrysis galbana* 25% C) throughout the rearing time.

2.2 Experimental setup

Toxicokinetic experiments

Two separate experiments were performed, one with CVs and one with CIIIs. Both were run in a flow-through rig system with eight chambers for exposure and four controls (5 L borosilicate flasks) featuring continuous renewal of the exposure solutions (SI: Figure S 1). Stock oil droplet dispersions of the weathered North Sea crude oil Troll B (200 °C+ residue) was created by the turbulence system described by Nordtug *et al*.[19] Oil droplets were removed by filtration to generate the WSF used as exposure medium (SI: Text section 1). The nominal and measured concentrations of oil in the dispersions, as well as the flow rates, number of individuals and durations for each experiment are given in Table 1. Different numbers of individuals were used due to the minimum requirements of material for tissue analysis and a difference in biomass between the two stages (CV: 12.0 ± 1.7 and CIII: 0.52 ± 0.28 mg wet weight/individual). At the end of the exposure period (4 or 8 d, Table 1), the animals were temporarily taken out of the rig and put back in clean containers, where they received clean seawater throughout the recovery period (20 or 35 d). No feed was provided during the exposure period. The CVs were not fed during the recovery period whereas the CIIIs were continuously fed with microalgae (*R. baltica*, 150 µg C/L) to prevent mortality due to energy loss.

Table 1. Details of the experimental setup. Nominal and measured concentration of oil (mg/L) in the stock oil droplet dispersion, average flow of filtered dispersion to the exposure chambers (mL/min), number of individuals in each exposure chamber (n), duration of the exposure and recovery periods (days).

Stage	Nominal conc. (mg/L)	Measured conc. (mg/L)	Flow (mL/min)	n per chamber	Days of exposure	Days of recovery
CV	1.0	1.00 ± 0.02	17.7 ± 0.97	25	8	35
CIII	0.75	0.51 ± 0.007	17.1 ± 0.80	330	4	20

Acute toxicity

The acute toxicity of the oil was evaluated using a modified ISO 14669:1999[20] including lower temperature (2±2 °C), an extended duration (8 d) for both stages, and a larger volume (2 L) for the CV stage. The exposure media were dilution series of water accommodated fraction (WAF) of Troll B 200 °C+ residue at an oil:water ratio (OWR) of 1:100. The test concentrations ranged from 12% to 100% WAF, where the 100 % was undiluted stock WAF. Static exposure was applied using 3 parallels for each WAF concentration and 6 controls, containing 7 copepods each. Immobilization was monitored daily (8 d). The initial 100% WAF stock and the 100 % and 12% WAF after exposure were sampled for exposure verification by chemical analyses (See SI: Text section 6).

2.3 Sampling and analyses

Exposure characterization

Oil droplet size distribution and concentration in the stock oil droplet dispersions was monitored daily by Coulter Counter (Multisizer 3, with 100 µm aperture). Samples of stock dispersion (20 mL) were siphoned from the settling chamber immediately before analyses. Samples of the exposure media were taken twice during each exposure period in the kinetics experiment for analyses of volatile organic compound (VOC, 40 mL, n=48) (SI: Table S 1), semi volatile organic compound (SVOC, 800 mL, n=48), and total extractable material (TEM). In the acute toxicity experiment, the initial 100 % WAF was sampled. All samples were acidified (pH<2) and stored in the dark at 2 °C. VOC in the C_5 to C_{10} range were determined directly in septum-capped vials by Purge and Trap (P&T) GC/MS using a modification of EPA method 8260C (US EPA,[21] SI: Table S 2). The SVOC samples were extracted in dichloromethane prior to analysis using GC/MS (gas chromatography/mass spectrometry) following a modified EPA Method 8270D (US EPA,[22] SI: Table S3). Total extractable material (TEM) in the same extracts were analysed using GC/FID according to a modification of US EPA Method 8100.[23] More details on sample preparations and analyses are given in SI: Text section 2.

Body residue of oil components

Samples for body residue (BR) analyses of SVOC were taken periodically during the exposure and recovery periods, along with three control groups in each setup (SI: Table S 1). Individual copepods

were imaged using a dissecting microscope (MZ APO; Leica Microsystems) equipped with a CCD camera (DS-Fi1; Nikon Inc., Japan) for biometrics. Subsequently, the individuals were carefully transferred to glass vials and frozen (-20 °C). Extraction of organic compound from homogenate of *C. hyperboreus* was performed as described in Sørensen *et al.*[24] (SI: Text section 2). Briefly, the samples were extracted in in *n*-hexane-dichloromethane, followed by a clean-up step to remove lipids using solid phase extraction (SPE). Internal standards were applied in two steps to quantify target compounds based on the average response factors (RF) of parent compounds. The final extract was analysed for 50 target compounds using GC-MS (SI: Table S 4).

Biometrics

Microscopy images of *C. hyperboreus* were analysed using ImageJ software,[25] where the free hand selection tool was used to determine regions of interest (ROI) along the perimeter of the prosome and the lipid sack (Figure S 2). The pixel-to-µm ratio was determined by measuring the pixel length of a calibration slide. The projected area and length of the prosome and the lipid sac was recorded, providing data for the calculation of prosome volume and lipid volume according to the formula:[26]

$$Volume = \pi \times \frac{Area^2}{4\,x\,Length} \qquad \text{(Eq. 1)}$$

2.4 Modelling and statistical analyses

One-compartment model

Uptake of dissolved components from the water phase into the tissue of an aquatic organism (body residue) can be modelled using a one-compartment model (see e.g.[6,27] and SI: Text section 3)

$$\frac{dC_i}{dt} = k_e(P_{iw}C_w - C_i) \qquad \text{(Eq. 2)}$$

The model parameters k_e (elimination rate) and P_{iw} (partitioning coefficient internal water, equivalent to the BCF) were estimated from measurements of body residues ($C_i(t)$) and exposure concentrations C_w. For constant exposure concentrations, the one-compartment model can be integrated analytically to yield the closed-form solution

$$C_i(t) = C_w P_{iw}\left(1 - e^{-k_e t}\right) + C_i(0)e^{-k_e t} \qquad \text{(Eq. 3)}$$

Exposure concentrations for individual oil components were measured and given in µg/L, body concentrations of oil component in µg/g and time in days. The model parameters are in units of 1/d (k_e) and L/kg (P_{iw}). The uptake rate (k_u) was calculated from the estimated model parameters: $k_u = k_e \times P_{iw}$, and the half-time of elimination ($T_{1/2}$) from k_e: $T_{1/2} = \ln 2/k_e$. No transformation was applied. Water concentrations were below the detection limit (SI: Table S3) for a few components in some of the exposure containers. Using the median water concentration over all exposure containers allowed us to estimate P_{iw} and k_e for all compounds. Body residue data that could not be analytically integrated due to baseline noise was set to zero, while values between zero and the detection limit were included in the model fits. Only the components with a sufficient number of detected data to fit models in both stages were included (26 out of 50 target compounds). The OMEGA model[6] was run with elimination to water only for both species, and with elimination by water and growth dilution for the CIII stage. For growth dilution, an exponential growth rate (k_g=0.040 d^{-1}) for the CIIIs was based on the average weight (w) of the individuals sampled for body residue analyses at intervals between t=0 and t=25 d ($w = w_0 \times e^{k_g \times t}$; SI: Figure S5).

Parameter estimation

Parameter values of k_e and P_{iw} for each component were estimated by minimizing the negative log-likelihood function with a non-linear optimization method using Eq. 3 (Nelder-Mead). The body residue data showed cases of initial body residues above zero at t=0, and stabilization at non-zero concentration during the depuration phase for some components (SI: Text section 7). Thus, the initial body residue (C_0) and exposure concentration during the recovery phase (C_{wrec}) were included as free parameters for the CIII estimations. For the CVs, C_0 and C_{wrec} were fixed at zero. Constant body volumes were assumed. Model parameters are given in SI: Table S 5.

Confidence intervals for the point estimates were calculated using the Markov chain Monte Carlo (MCMC) method to sample the posterior, where we used uninformative top-hat priors, non-zero on the finite interval [1e-7, 1e2]. The MCMC simulations were run for 33000 steps, using 8 walkers, and a burn-in of 3000 steps. Every 5th step was kept, resulting in 6000 steps. From this final sample, 5 and 95 percentile values were reported. Samples from the posterior (600) were used to give intervals on the model predictions for $C_i(t)$, plotted over the best fit line and data points (SI: Text section 7). Some of the low-K_{OW} compounds in the CIII data exhibited non-converging elimination rate (k_e) MLE values and profiling the (negative log-) likelihood function indicated a weak (or no) minimum. In these cases, the upper end of the prior function top-hat was lowered to 10 1/h, to improve the convergence of the MCMC simulations and obtain a better estimate for the lower end of the CI.

Statistical analyses and software

Parameter estimates where performed in Python using the lmfit package,[28] in conjunction with scipy, numpy and pandas. The MCMC simulations where performed with emcee.[29] Statistical analyses were performed using R [30] and GraphPad Prism V6.00 (GraphPad Software, Inc., CA, USA). Analyses of variance (ANOVA) with multi-comparison test (TukeyHSD) were used to compare means of groups. Statistical significance level was set to $p<0.05$. Four-parameter logistic regressions were applied to the time-dependent mortality data. Figure 1 and 2 where produced with Python matplotlib and pandas, figure 3 in GraphPad Prism.

3 Results and discussion

3.1 Toxicokinetics

Uptake of oil components

The body concentrations were close to steady state in the lipid-poor CIIIs at the end of the exposure phase, whereas most components were far from steady state in the CVs (Figure 1 and SI: Text section 7). The concentrations of low K_{OW} components (log K_{OW}<4.5) were lower in the CIIIs than in the CVs after 4 d exposure to WSF (Figure 1). This was in line with the lower exposure concentration in the CIII experiment (SI: Figure S 10), and the expectations of higher body concentrations of organic compounds in organisms with high lipid content.[27] Surprisingly, with increasing lipophilicity of the oil components, we observe a shift in this pattern (Figure 1). For the larger and more alkylated compounds, like chrysenes and phenanthrenes, the body concentrations were up to three-fold higher in the CIIIs than in the CVs after 4 d of exposure. This pattern persisted even after 8 d exposure of the CVs, indicating that the uptake of high K_{OW} components must be faster in the CIIIs than in the CVs. The uptake rate constants (K_u, L/kg/day) were higher for the CIIIs than for the CVs (Figure 2), with an increasing divergence with increasing K_{OW} (SI: Figure S 5). According to Hendriks *et al.*, k_u does not depend directly on the f_L of the organism but is dependent on its body mass and the K_{OW} of the chemical.[6] Hence, the smaller size of the CIIIs compared to the CVs (Figure S 3) may explain the higher body concentrations of the most lipophilic oil components in the CIIIs compared to the CVs at the end of the exposure phase.

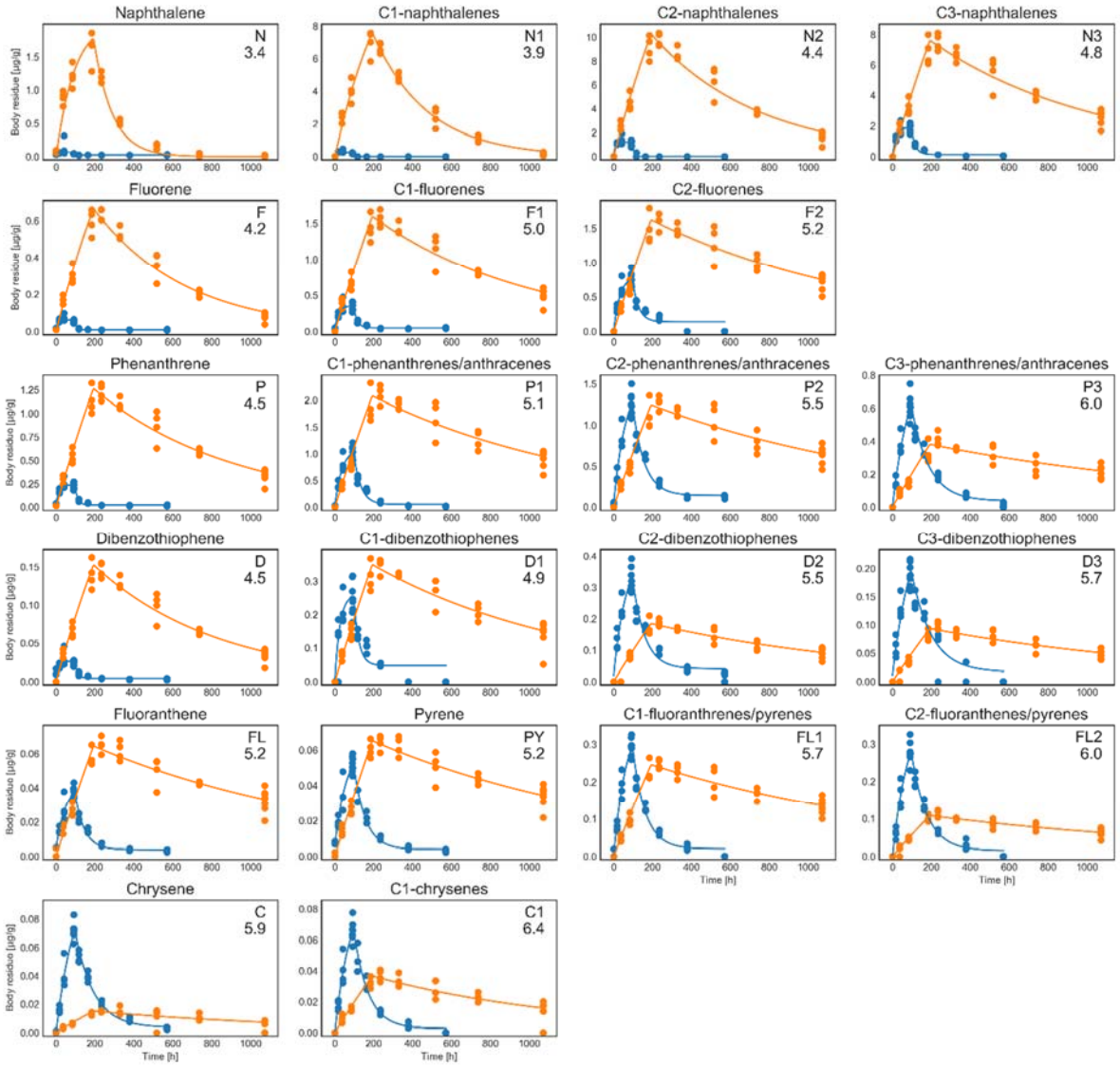

Figure 1. Body residues (µg/g wet weight) of oil components in *C. hyperboreus* after exposure to crude oil water soluble fraction (WSF) for 8 or 4 d, followed by 35 or 20 d recovery for lipid-rich (orange) and lipid-poor (blue) copepods. Best fit lines from one-compartment models, see text and SI: Text section 7 for details. Numbers are log K_{OW}. Model fits for all components are shown in SI: Text section 7.

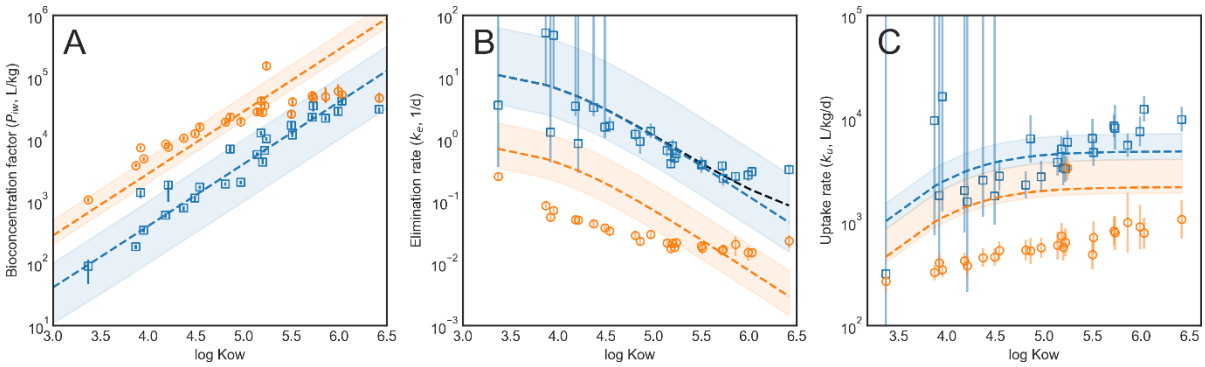

Figure 2. Bioconcentration factors (A; log P_{iw}, L/kg), elimination rates (B; log k_e, 1/d) and uptake rates (C; k_u, L/kg/d) as function of octanol-water partitioning coefficients (log K_{OW}) for 26 oil components in lipid-rich CV (orange circles) and lipid-poor CIII (blue squares) *C. hyperboreus* exposed to the water-soluble fraction (WFS) of crude oil. P_{iw} and k_e are estimated from one-compartment models fitted to body concentration data, k_u is calculated as k_e x P_{iw}. Error bars: 95% CI from the MCMC posterior, see section 2.4. The lines are predictions from the OMEGA model for the mean weight (0.5 and 12.5 mg) and estimated lipid content (5% and 28%) of the two stages. Shaded area indicates the realistic range for each stage in the present study (CIII: weight 0.1 – 1, lipid: 1 – 10%; CV: weight 1-20 mg, lipid: 20 – 50%). The black line in 2B includes the growth dilution term of the OMEGA model[6] for the CIII stage.

Bioconcentration factors (BCFs)

The one-compartment model (Eq. 3) was used to estimate steady-state BCFs for 26 oil components (Figure 2 and SI: Table S 5). The BCFs ranged 90-59 000 and 1000-180 000 L/kg wet weight for CIIIs and CVs, respectively. The bioconcentration potential was clearly higher in the lipid-rich CVs than in the CIIIs, as expected from the assumption that the lipid content is the main predictor of the partitioning of lipophilic oil components between organisms and water. The OMEGA bioaccumulation model[6] was used to predict BCFs for oil components based on the average body mass and lipid content of each stage (Figure 2 and Section 3.2). In addition to the prediction lines for the specific weight and lipid content, the shaded areas give the realistic ranges of weight and lipid content for each stage (see Figure 2 for details). For the lipid-poor CIIIs, our estimated BCFs are well in line with the predictions from the OMEGA model over the full range of K_{OW} (Figure 2). The OMEGA prediction for the CIIIs was based on 5 % lipid, which is higher than the volume-based lipid fractions estimated from the relative size of the lipid sac (see section 3.2). The OMEGA prediction for the CIIIs are the same as the Mackay regression, which assumes 4.8 % lipid content of the organism,[7] and we assume 5% to be a reasonable lipid content of the structural fraction. For the CVs, our BCFs fits less well to the OMEGA prediction, and are levelling off at K_{OW} >5 (Figure 2). A lipid content of 28% is used as input to the OMEGA model for this stage (Figure S 3), which results in an underestimation of the BCFs at the lower range of log K_{OW}. The total lipid fraction is probably higher than 28%, as the lipid of the structural tissue is not included (See section 3.2). In general, models predicting log BCF from log K_{OW} are linear with a slope of 1 in the log K_{OW} range 2-6[6, 10, 31, 32]. Deviations from such a linear relationship have been reported for K_{OW} <2 and >6, which has been attributed to lower bioavailability of high K_{OW} compounds, association of oil components with proteins, and biotransformation and active excretion.[4-6]

The bioavailability of oil components is expected to have been similar in both experiments. The experiments were performed in a flow-through rig system with continuous renewal of the exposure solutions preventing the depletion of oil components that can be observed in static systems. Nevertheless, factors influencing the bioavailability of dissolved oil components may have been present. Oil components will associate with dissolved organic carbon (DOC) in the seawater, reducing their bioavailability.[33] Pre-filtering seawater (1 µm) will not prevent natural DOC from entering the exposure system, potentially leading to an overestimation of the bioavailable fraction based on the total water concentration. DOC levels may have differed between the experiments, which could explain the levelling off of the BCFs for the CVs (Figure 2). However, it is more likely that the DOC concentration was higher during the CIII experiment, as June is a more productive period than

September. The reduced BCF values for very lipophilic compounds in CV is therefore unlikely caused by a substantially lowered bioavailability.

Biotransformation of oil components is believed to be of minor importance in zooplankton[4, 6]. However, Jensen *et al*[34] suggested biotransformation or active excretion as the cause of BCFs lower than the K_{OW} for phenanthrene and benzo[a]pyrene in *Calanus finmarchicus*. Transcripts of enzymes that may biotransform organic contaminants has been found in *Calanus* spp[35], but the significance of these enzymes in the elimination of organic contaminants is unknown. If biotransformation or active excretion occurs to some extent, it may have differed between the stages, however, this is not assumed to be an explanation for the dissimilar BCF patterns (Figure 2).

The lack of coherence in the log K_{OW}-log BCF relationships between the two stages (Figure 2) is interesting and difficult to explain. Since the K_{OW} describes the partitioning between water and an organic phase, we expected that it would be a better predictor of accumulation of oil compounds in the lipid-rich stage compared to the lipid-poor stage. This given the assumption that highly lipophilic organic compounds will partition mainly to the lipid compartment of an organism[7]. One explanation may be a difference in relative lipid composition between the two stages. Lipids will be found in both the structural compartment (e.g. as membrane lipids) and in the discrete lipid sac as energy storage containing mainly wax esters[22, 26]. The lipid composition of the structural tissue is believed to be similar in the two stages, but the CVs had considerably larger lipid sacs than the CIIIs (Figure S 3). This implies that the wax esters will dominate the total lipid fraction of the CVs, whereas they may be of minor importance in the CIIIs. The lipid of the structural fraction may be more similar to octanol than the wax esters of the lipid sac, causing a poor estimation of BCF based on K_{OW} when the wax esters are dominating over the structural lipids. To further understand the relative contribution of all these mechanisms more research is needed.

Elimination of oil components

The body concentration of oil components immediately started to decrease after transfer from the exposure media to clean seawater (Figure 1). In the CIIIs, most of the components were eliminated down to background levels after 20 d recovery. In contrast, only the low K_{OW} compounds naphthalenes (N-N1) and fluorene (F) were approaching background levels in the CVs after 36 d recovery (Figure 1 and SI: Text section 7). Most of the oil components were retained in the body of the CVs in levels up to 68% of the maximum concentrations (8 d exposure) after the recovery period. The retention of oil

components increased with increasing K_{OW} (Figure 2). The half-times were all below 3 days for the CIIIs, whereas for the CVs the half-times ranged between 3.5 and 47 days (SI: Fig. 6).

The elimination rates (k_e) are expected to decrease with increasing K_{OW}, as well as with increasing body mass and lipid fraction of the organism[4]. Our estimated k_es are plotted against OMEGA predictions of elimination rates in Figure 2. The lower k_es for the CVs compared to the CIIIs was expected based on the differences in size and lipid content (Figure S 3). For the CIIIs, the k_es generally follows the prediction of the OMEGA model, except for a levelling off for the most lipophilic components (log K_{OW} > 6). It should, however, be noted that the uncertainties of the k_es for the low K_{OW} components are relatively high for the CIII, illustrated by the wide error bars (Figure 2). For these components, the uptake is so fast that steady state is reached within the first day of exposure. The elimination is equally fast, making it difficult to estimate parameters with high certainty. The slower kinetics of the CVs reduce the uncertainty in the estimates of k_e markedly. Still, most of our k_e values for the CVs are outside the realistic range of weight (1-20 mg) and lipid fraction (20-50%; Figure 2). For all components with log K_{OW} <5, there is an overestimation of the k_e by approximately half an order of magnitude by the OMEGA model relative to our k_es. Similar deviations from model predictions has been demonstrated for lipid-rich eels (*Anguilla anguilla*) accumulating organochlorine compounds. [36] The k_e-log K_{OW} relationship also levels of for the CVs, but it seems to be initiated at lower K_{OW} (approx. log K_{OW}<5) than for the CIIIs. The relatively poor performance of OMEGA for the CV may be caused by several factors, such as dormancy and lipid storage, discussed in detail in the next section.

3.2 Lipid content, body size and confounding factors

The copepodite stages three (CIII) and five (CV) of *C. hyperboreus* were expected to differ in lipid content, as this gradually increases in the late copepodite stages (CIII-CV).[37] This was verified by volume-based lipid content of 0.40 % for CIII and 28.7 % for CV (day zero; Figure S 3). Our estimated lipid fractions are based on the calculated volume of the lipid sac (Eq. 1), which will be lower than the total lipid volume of the individual, as the lipids in the structural tissue is not accounted for. Using the two-dimensional area of the lipid sac may also bias the lipid volume estimates, since the actual three-dimensional shape of the lipid sac is unknown. By back-predicting the average lipid fraction from the estimated partitioning coefficient P_{iw} (Table S 5), using the assumption that $f_L = P_{iw}/K_{OW}$ and all data, we find an average total lipid content of 5.0 ± 3.4 % and 31.4 ± 24.2 % for the lipid-poor and lipid-rich *C. hyperboreus*, respectively. For the CVs, the log P_{iw}-log K_{OW} regression was only linear for log K_{OW}<5,5 (Figure 2), and by excluding the P_{iw}s for log K_{OW}>5.5, we obtain an estimated lipid content of 42.7 ± 18.2 %. Weight based lipid contents of CV and adult female *C. hyperboreus* determined gravimetrically after organic extraction is reported in the range 40-65 and 15-62 % dry weight, respectively [38, 39].

Conversion between the methods require knowledge of density and wet weight/dry weight ratios and is not straight forward. Lipid fractions for CIII *C. hyperboreus* has, to our knowledge, not previously been reported.

The stage distribution of the copepods changed during the experimental period (SI: Figure S 11), which had implications for the size and relative lipid volume (SI: Figure S 3). The lipid volume of the lipid-rich copepods decreased from d 8 to d 45 ($p<0.001$), while the prosome volume was constant, resulting in a reduced lipid fraction (Figure S 3). The change in lipid content was accompanied by a transition from CV to adult females, which was the dominating stage at the end of the recovery (45d). The lipid compartment of the CVs had most likely been redistributed or used as an energy source to pay maintenance costs and produce eggs in the females[15]. The lipid-poor copepods where fed in the recovery phase and therefore gradually increased in size throughout the 24d experimental period with an exponential growth rate of 0.040/day (SI: Figure S 3A and 4). This was accompanied by a gradual transformation from CIII to CIV (SI: Text section 5). The CIVs had a significantly higher lipid volume fraction compared to the CIIIs (3.3 ± 0.6 and 0.9 ± 0.16 %, respectively; t-test, $p<0.001$), although large variation within each stage was observed. Despite CIVs comprising 40% of the lipid-poor copepods at 4 d, a significant increase in relative lipid volume was not observed until day 24 (SI: Figure S 3B). This may be due by a time lag in the build-up of lipid stores after moult.

The main change in relative lipid volumes occurred after the exposure periods in both experiments (SI: Figure S 3). Hence, it is not believed to have influenced the uptake rate of the oil components. The growth and/or the changes in lipid volume may, however, have had implications for the interpretation of the data from the recovery period. Decreasing lipid volumes of the CVs during the recovery period may have increased the depuration of oil components, causing an overestimation of the k_es in the lipid-rich CVs. In the CVs, oil components were generally far from steady state after the exposure period (SI: Text section 7), meaning that the parameter estimation rests on the data for the depuration phase. As the estimation of the BCF (P_{iw}) is strongly dependent on the k_e (Eq.3), overestimated k_es may have given rise to underestimated BCFs for the CVs. This effect will increase with increasing K_{OW}, as the more lipophilic components are further from steady state. For the CIIIs, the increased growth and lipid accumulation (SI: Figure S 3) may have resulted in overestimated k_es due to biodilution during the recovery period. However, the OMEGA prediction including dilution by growth in addition to elimination to water[6] show that growth dilution has a very limited effect on the ke estimation and do not explain the levelling off of the k_es (Fig 2B, black line).

The activity level of the CIIIs and CVs differed during the exposure period, which may have been influencing the oil component accumulation. The CVs were in apparent diapause (slow and dormant) during the exposure period (d 0-8), while the CIIIs were active. In the dormant state, the metabolism of *C. hyperboreus* is reduced. [38] The reduced oxygen demand and low activity of the CVs potentially reduced the exchange of chemicals between the body and the exposure medium. This may be one explanation for the overestimation of uptake rates by the OMEGA model for the CVs (Figure 2). As the experiment progressed, the activity level of the CVs increased. Hence, the elimination of oil components may have been less affected than the uptake rates. However, the elimination rate parameters of our models are based both on the uptake and the depuration kinetics, so we cannot exclude the possibility of a bias caused by the activity level of the CVs.

3.3 Acute toxicity of dissolved oil components

Our acute toxicity experiments show that WAF of the crude oil was considerably more toxic to the lipid-poor than to the lipid-rich copepods, as indicated by the estimated LC_{10} of 1.2 and 2.1 mg/L TEM after 8 d exposure, respectively (Figure 3 and SI: Text section 6). A mortality exceeding 50% was reached by the CIIIs after 5 d, whereas only partial mortality (15%) was observed for the CVs after 8 d (Figure 3). Based on the differences in sensitivity to acute WAF exposure, the exposure concentration of the CIIIs was set to 50 % of the level of the exposure of the CVs in the kinetics experiments. Lipids are suggested to offer protection from toxicity of organic compounds[40], but recent works have shown that this is unlikely to be the full explanation when it comes to copepods and oil components[19, 20]. Lipids will have contributed to the observed toxicity patterns, as lipid-rich copepods had lower k_e values and thus reach steady state more slowly (which could delay the onset of toxic effects). Other factors including body size, activity and intrinsic sensitivity differences between stages are likely contributing to the apparent difference in sensitivity between the stages. For a better understanding of the processes leading to increased sensitivity in the lipid-poor stage, two-compartment models may be useful. Modelling the concentrations in both the structural compartment and the lipid compartment simultaneously could give predictions of how fast the structural compartment reaches toxic concentrations (see e.g., Jager *et al.*[27]). This cannot be deducted from total body concentrations and one-compartment models for lipid-rich stages.

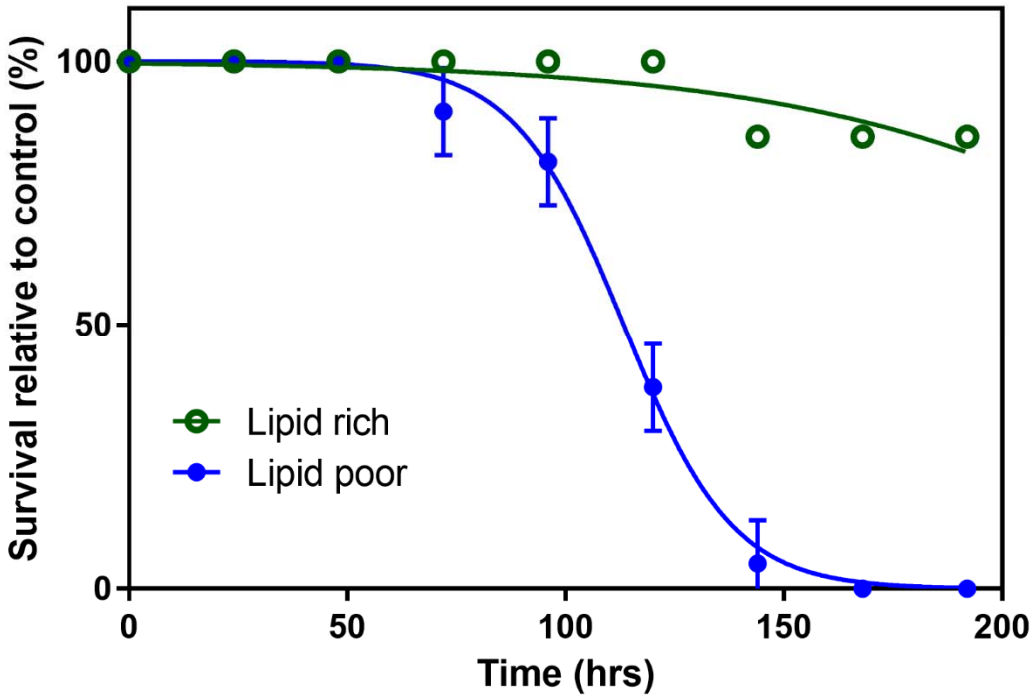

Figure 3. Survival as a function of exposure time for lipid-poor (blue) and lipid-rich (green) copepodite stages of *Calanus hyperboreus* exposed 100% WAF of oil:water ratios of 1:100 of artificially weathered Troll B crude oil (200 °C + residue). The total concentration of oil components (TEM) in the exposure solutions were 2.6 mg/L and 2.1 mg/L for the tests with lipid rich and lipid poor stages, respectively. The trend lines were obtained by four-parameter logistic regression, where the top and bottom plateaus were set to 0 and 100%. Lipid-poor R^2= 0.987, lipid-rich R^2=0.753.

3.4 Implications for risk assessments

In general, there were good agreements between our parameter estimates for the lipid-poor stage and the QSAR predictions made by the OMEGA model (Figure 2). For the lipid-rich stage, the BCF predictions by the OMEGA model fitted reasonably well with our data, except for the levelling off at log KOW >5. This means that overall the OMEGA model captures the bioaccumulation potential of oil components in both stages of *C. hyperboreus.* In contrast, for the lipid-rich CVs we observe a misfit of about half an order of magnitude between our estimated uptake (k_u) and elimination (k_e) rates relative to the OMEGA predictions (Figure 2). This implies that the elimination of oil components will take approximately 3-4 times longer than predicted by the model (SI: Figure S6), leading to an underestimation of potential long-term effects by the current QSAR approach. On the other hand, the uptake for oil components in the lipid-rich copepods will be equally delayed relative to the model predictions, leading to an overestimation of potential acute effects of oil components after an oil spill. The complex situation of the lipid storage in *C. hyperboreus* may be captured by applying correction

449 factors to the current QSAR models. However, to ensure more accurate environmental risk
450 assessment by QSAR models for Arctic areas, the mechanisms causing the misfit for the lipid-rich stage
451 should be further elucidated.

452 The uptake and elimination kinetics followed one-compartment behaviour for both stages (Figure 1
453 and SI: Text section 7). Two-compartment behaviour was expected, at least for the lipid-rich CVs,
454 considering the discrete lipid storage and the recent identification of two-compartment kinetics in the
455 related *C. finmarchicus*.[27] Although one-compartment models provide useful estimates of parameters
456 for total body concentrations, two-compartment models predicting concentrations in the structural
457 tissue and lipid storage separately may be better predictors of toxic effects. We did attempt to fit two-
458 compartment models to the CV data, but the parameters could not be identified. Two-compartment
459 models include more parameters to be estimated, which in turn require more input data to the
460 models.

461 The long retention time of oil components in the lipid storage of *C. hyperboreus* (Figure 2) may have
462 implications during diapause and gonad maturation when the lipid store is utilized.[41] The potential
463 transfer of oil components to offspring through the incorporation of contaminants in lipid rich eggs is
464 of particular concern in *C. hyperboreus*, which has more lipid rich eggs than *C. finmarchicus* and
465 *Calanus glacialis*[42]. In addition, the potential for food web transfer of oil components are largely
466 increased by the long retention time. These aspects are important for environmental risk assessment
467 in the Arctic, where lipid-rich copepods dominate the zooplankton communities.

468

469 Acknowledgements: The research presented in this article was funded by Statoil Petroleum and SINTEF
470 Ocean, Norway. We would like to thank Iurgi Salaberria (NTNU) and Torkel Gissel Nielsen (DTU), as
471 well as the locals in Qeqertarsuaq for field collection of copepods in Greenland, and Lisbet Sørensen
472 and the laboratory staff at SINTEF Ocean for the chemical analyses. Statoil is acknowledged for their
473 comments on the draft manuscript.

474 Supporting information: The supporting information includes additional descriptions of methods,
475 compound targets lists and analytical results, parameter estimates and model fits for all 26
476 components, and extended results for the stage distribution and acute toxicity.

477 4 References

478

479 1. Olsvik, P. A.; Hansen, B. H.; Nordtug, T.; Moren, M.; Nolen, E.; Lie, K. K., Transcriptional evidence
480 for low contribution of oil droplets to acute toxicity from dispersed oil in first feeding Atlantic cod

(*Gadus morhua*) larvae. *Comparative Biochemistry and Physiology C-Toxicology & Pharmacology* **2011,** *154*, (4), 333-345.
2. Olsvik, P. A.; Nordtug, T.; Altin, D.; Lie, K. K.; Overrein, I.; Hansen, B. H., Transcriptional effects on glutathione S-transferases in first feeding Atlantic cod (*Gadus morhua*) larvae exposed to crude oil. *Chemosphere* **2010,** *79*, (9), 905-913.
3. Viaene, K. P.; Janssen, C. R.; de Hoop, L.; Hendriks, A. J.; De Laender, F., Evaluating the contribution of ingested oil droplets to the bioaccumulation of oil components—A modeling approach. *Science of The Total Environment* **2014,** *499*, 99-106.
4. Arnot, J. A.; Gobas, F. A. P. C., A review of bioconcentration factor (BCF) and bioaccumulation factor (BAF) assessments for organic chemicals in aquatic organisms. *Environmental Reviews* **2006,** *14*, (4), 257-297.
5. Grisoni, F.; Consonni, V.; Villa, S.; Vighi, M.; Todeschini, R., QSAR models for bioconcentration: Is the increase in the complexity justified by more accurate predictions? *Chemosphere* **2015,** *127*, (Supplement C), 171-179.
6. Hendriks, J.; van der Linde, A.; Cornelissen, G.; Sijm, D., The power of size. 1. Rate constants and equilibrium ratios for accumulation of organic substances related to octanol-water partition ratio and species weight. *Environmental Toxicology and Chemistry* **2001,** *20*, (7), 1399-420.
7. Mackay, D., Correlation of bioconcentration factors. *Environmental Science & Technology* **1982,** *16*, (5), 274-278.
8. Veith, G. D.; DeFoe, D. L.; Bergstedt, B. V., Measuring and Estimating the Bioconcentration Factor of Chemicals in Fish. *Journal of the Fisheries Research Board of Canada* **1979,** *36*, (9), 1040-1048.
9. Chapman, P. M.; Riddle, M. J., Toxic Effects of Contaminants in Polar Marine Environments. *Environmental Science & Technology* **2005,** *39*, (9), 200A-206A.
10. de Hoop, L.; Schipper, A. M.; Leuven, R.; Huijbregts, M. A. J.; Olsen, G. H.; Smit, M. G. D.; Hendriks, A. J., Sensitivity of Polar and Temperate Marine Organisms to Oil Components. *Environmental Science & Technology* **2011,** *45*, (20), 9017-9023.
11. Olsen, G. H.; Klok, C.; Hendriks, A. J.; Geraudie, P.; De Hoop, L.; De Laender, F.; Farmen, E.; Grøsvik, B. E.; Hansen, B. H.; Hjorth, M.; Jansen, C. R.; Nordtug, T.; Ravagnan, E.; Viaene, K.; Carroll, J., Toxicity data for modeling impacts of oil components in an Arctic ecosystem. *Marine Environmental Research* **2013,** 90, 9-17.
12. Agersted, M. D.; Møller, E. F.; Gustavson, K., Bioaccumulation of oil compounds in the high-Arctic copepod *Calanus hyperboreus*. *Aquatic Toxicology* **2018,** *195*, 8-14.
13. Nørregaard, R. D.; Nielsen, T. G.; Møller, E. F.; Strand, J.; Espersen, L.; Møhl, M., Evaluating pyrene toxicity on Arctic key copepod species *Calanus hyperboreus*. *Ecotoxicology* **2014,** *23*, (2), 163-174.
14. Hobson, K. A.; Welch, H. E., Determination of trophic relationships within a high Arctic marine food web using δ 13 C and δ 15 N analysis. *Marine Ecology Progress Series* **1992**, 84, 9-18.
15. Hirche, H.-J., Life cycle of the copepod *Calanus hyperboreus* in the Greenland Sea. *Marine Biology* **1997,** *128*, (4), 607-618.
16. Falk-Petersen, S.; Mayzaud, P.; Kattner, G.; Sargent, J. R., Lipids and life strategy of Arctic *Calanus*. *Marine Biology Research* **2009,** *5*, (1), 18-39.
17. F., L. R.; Wilhelm, H.; Gerhard, K., Lipid storage in marine zooplankton. *Marine Ecology Progress Series* **2006,** *307*, 273-306.
18. Hansen, B. H.; Tarrant, A. M.; Salaberria, I.; Altin, D.; Nordtug, T.; Øverjordet, I. B., Maternal polycyclic aromatic hydrocarbon (PAH) transfer and effects on offspring of copepods exposed to dispersed oil with and without oil droplets. *Journal of Toxicology and Environmental Health, Part A* **2017,** *80*, (16-18), 881-894.
19. Nordtug, T.; Olsen, A. J.; Altin, D.; Meier, S.; Overrein, I.; Hansen, B. H.; Johansen, Ø., Method for generating parameterized ecotoxicity data of dispersed oil for use in environmental modelling. *Marine Pollution Bulletin* **2011,** *62*, (10), 2106-2113.

20.ISO *ISO 14669:1999 - Water quality - Determination of acute lethal toxicity to marine copepods (Copepoda, Crustacea).* 1999.
21.USEPA, Method 8260C: Volatile organic compounds by gas chromatography/mass spectrometry (GC/MS). **2006**.
22.USEPA, Method 8270D: Semivolatile Organic Compounds by GC/MS. **2007**.
23.USEPA, Method 8100: Polynuclear aromatic hydrocarbons. **1986**
24.Sørensen, L.; Silva, M. S.; Booth, A. M.; Meier, S., Optimization and comparison of miniaturized extraction techniques for PAHs from crude oil exposed Atlantic cod and haddock eggs. *Analytical and bioanalytical chemistry* **2016,** *408*, (4), 1023-1032.
25.Rasband, W. imageJ http://imagej.net/index.html
26.Miller, C. B.; Morgan, C. A.; Prahl, F. G.; Sparrow, M. A., Storage lipids of the copepod *Calanus finmarchicus* from Georges Bank and the Gulf of Maine. *Limnology and Oceanography* **1998,** *43*, (3), 488-497.
27.Jager, T.; Øverjordet, I. B.; Nepstad, R.; Hansen, B. H., Dynamic links between lipid storage, toxicokinetics and mortality in a marine copepod exposed to dimethylnaphthalene. *Environmental Science & Technology* **2017,** *51*, 7707-7713.
28.Newville, M.; Stensitzki, T.; Allen, D. B.; Rawlik, M.; Ingargiola, A.; Nelson, A., LMFIT: non-linear least-square minimization and curve-fitting for Python. *Astrophysics Source Code Library* **2016**.
29.Foreman-Mackey, D.; Hogg, D. W.; Lang, D.; Goodman, J., emcee: The MCMC Hammer. *Publ. Astron. Soc. Pac.* **2013,** *125*, (925), 306-312.
30.R Core Team, R: A Language and Environment for Statistical Computing. In 3.4.3 ed.; R Foundation for Statistical Computing: Vienna, Austria, 2017.
31.Bechmann, R. K.; Larsen, B. K.; Taban, I. C.; Hellgren, L. I.; Møller, P.; Sanni, S., Chronic exposure of adults and embryos of *Pandalus borealis* to oil causes PAH accumulation, initiation of biomarker responses and an increase in larval mortality. *Marine Pollution Bulletin* **2010,** *60*, (11), 2087-2098.
32.Fisk, A. T.; Stern, G. A.; Hobson, K. A.; Strachan, W. J.; Loewen, M. D.; Norstrom, R. J., Persistent Organic Pollutants (POPs) in a Small, Herbivorous, Arctic Marine Zooplankton (*Calanus hyperboreus*): Trends from April to July and the Influence of Lipids and Trophic Transfer. *Marine Pollution Bulletin* **2001,** *43*, (1), 93-101.
33.Landrum, P. F.; Nihart, S. R.; Eadie, B. J.; Herche, L. R., Reduction in bioavailability of organic contaminants to the amphipod pontoporeia hoyi by dissolved organic matter of sediment interstitial waters. *Environmental Toxicology & Chemistry,6,* **1987**, (1), 11-20.
34.Jensen, L. K.; Honkanen, J. O.; Jæger, I.; Carroll, J., Bioaccumulation of phenanthrene and benzo[a]pyrene in *Calanus finmarchicus*. *Ecotoxicology and Environmental Safety* **2012,** *78*, (Supplement C), 225-231.
35.Hansen, B. H.; Altin, D.; Nordtug, T.; Olsen, A. J., Suppression subtractive hybridization library prepared from the copepod *Calanus finmarchicus* exposed to a sublethal mixture of environmental stressors. *Comparative Biochemistry and Physiology Part D: Genomics and Proteomics* **2007,** *2*, (3), 250-256.
36. de Boer, J.; van der Valk, F.; Kerkhoff, M. A. T.; Hagel, P.; Brinkman, U. A. T., An 8-Year Study on the Elimination of PCBs and Other Organochlorine Compounds from Eel (*Anguilla anguilla*) under Natural Conditions. Environmental Science & Technology 1994, 28, (13), 2242-2248.
37.Scott, C. L.; Kwasniewski, S.; Falk-Petersen, S.; Sargent, J. R., Lipids and life strategies of *Calanus finmarchicus, Calanus glacialis* and *Calanus hyperboreus* in late autumn, Kongsfjorden, Svalbard. *Polar Biology* **2000,** *23*, (7), 510-516.
38.Auel, H.; Klages, M.; Werner, I., Respiration and lipid content of the Arctic copepod *Calanus hyperboreus* overwintering 1 m above the seafloor at 2,300 m water depth in the Fram Strait. 2003; Vol. 143, p 275-282.
39.Lee, R. F., Lipid composition of the copepod *Calanus hyperboreas* from the Arctic Ocean. Changes with depth and season. *Marine Biology* **1974,** *26*, (4), 313-318.

40.Lassiter, R. R.; Hallam, T. G., Survival of the fattest: Implications for acute effects of lipophilic chemicals on aquatic populations. *Environmental Toxicology and Chemistry* **1990,** *9*, (5), 585-595.
41.Hansen, B. H.; Jager, T.; Altin, D.; Øverjordet, I. B.; Olsen, A. J.; Salaberria, I.; Nordtug, T., Acute toxicity of dispersed crude oil on the cold-water copepod *Calanus finmarchicus*: Elusive implications of lipid content. *Journal of Toxicology and Environmental Health, Part A* **2016,** *79*, (13-15), 549-557.
42.Jung-Madsen, S.; Nielsen, T., Early development of *Calanus glacialis* and *C. finmarchicus*: Early development of Arctic *Calanus* spp. 2015; Vol. 60. DOI: 10.1002/lno.10070